Monitoring lithographic focus and tilting performance by off-line overlay measurement tools

Chin-Yu Ku, Tan Fu Lei, and Dong-Shieh Cheng

Citation: Journal of Vacuum Science & Technology B **19**, 1915 (2001); doi: 10.1116/1.1404978
View online: http://dx.doi.org/10.1116/1.1404978
View Table of Contents: http://scitation.aip.org/content/avs/journal/jvstb/19/5?ver=pdfcov
Published by the AVS: Science & Technology of Materials, Interfaces, and Processing

Monitoring lithographic focus and tilting performance by off-line overlay measurement tools

Chin-Yu Ku and Tan Fu Lei[a)]
Department of Electronics Engineering and Institute of Electronics, National Chiao Tung University, 1001 Ta Hsueh Road, Hsinchu 300, Taiwan, Republic of China

Dong-Shieh Cheng
Vanguard International Semiconductor Corporation, Hsinchu 300, Taiwan, Republic of China

(Received 30 January 2001; accepted 30 July 2001)

In this work we present a novel bar-in-bar (BIB) pattern to monitor the focus and tilting of exposure tools and production wafers. The inner and outer bars contain various hole sizes. When defocused, the shrinkage of the smaller patterns is more significant than that of the larger ones, thus causing the center of gravity to shift. Through the organization of the bar patterns, the centers of inner and outer bars shift in opposite directions when defocused. An overlay measurement tool can be used to easily measure the shift between the centers of inner and outer bars. Therefore, a second-order polynomial equation can precisely fit the measured BIB shift. In addition, an accurate and reliable focus value can be obtained with a maximum error of less than 0.05 μm by simply differentiating the fitting equation. The novel BIB has many applications, such as measuring field curvatures for exposure tools and determining best focus related information for production wafers. © *2001 American Vacuum Society.* [DOI: 10.1116/1.1404978]

I. INTRODUCTION

Accurately and reliably determining the best focus, tilting, and field curvature has become increasingly important due to the decreasing depth of focus (DOF) of modern high numerical aperture (NA) lithographic tools. Considerable attention has been paid to more precisely measuring the position of best focus.[1–10] A conventional focus measurement technique exposes a focus energy matrix (FEM) wafer, where each exposure field uses different focuses and energy offsets. The best focus can be obtained at the selected energy by a scanning electron microscope (SEM) after developing the wafer. However, recent progress in photoresist (PR) has made it difficult to determine the best focus by SEM measurement of the PR linewidth because PR retains nearly the same linewidth over a wide range of defocus. Another feasible convenient technique for determining the best focus uses focus dot arrays to create patterns that can be read by the naked eye.[11] However, this technique is less quantitative, with an error about $\pm$ 0.1 μm, and is inadequate for advanced lithographic tools. The phase shifting mask[12–18] (PSM) can quickly and accurately measure the best focus by employing an overlay measurement system.[19,20] However, we have found that this technique is difficult to construct in the laboratory when utilizing a commercialized focus monitor reticle. The procedural failure may be attributed to the complicated nature of the PSM process which is sensitive to machine settings and a shifter angle.[14–16] According to another study, the best focus can also be measured using the line end shortening effect, which is the rounding and shortening at the end of photoresist line pattern induced by light diffraction. Although this technology is simple and fast, its lack of accuracy impedes applications of advanced lithographic tools.[21,22]

In this study we describe a novel bar-in-bar (BIB) pattern to accurately determine the best focus for the most advanced lithographic tools. The BIB pattern is drawn on a conventional chrome binary mask to expose the inner and outer bars on the wafer simultaneously. The focus errors can be translated into the center shifts on the inner and outer bars. After the exposed wafer is developed, the shifts of the printed resist patterns can be conveniently measured by the off-line overlay measurement system. The center-to-center shift (referred to herein as ''overlay shift'') of the inner and outer bars under various focus settings can be characterized by a second-order polynomial equation. Thus, the best focus can be accurately and reliably determined by simply differentiating the fitting equation.

The BIB pattern designed herein can be inserted into the scribe lanes of the actual production mask, and printed simultaneously with the chip patterns. The shift of this novel BIB pattern can acquire the best focus related information if a FEM is performed.[21–26]

II. EXPERIMENTAL SETUP

A. Reticle design

Figure 1 displays the BIB layout proposed in our previous work.[1] Four columns of contact holes constitute each bar of the BIB. For the normal BIB pattern, the reticle is covered by a chrome film, and only the hole region (bar ''L'') is transparent enough to allow light to pass through the reticle (and vice versa for the reversed BIB pattern). The pattern sizes and layouts for normal and reversed BIB shown in Fig. 1 were optimized to be best fitted by a second-order polynomial equation. The BIB pattern was used to measure the best

a)Electronic mail: tflei@cc.nctu.edu.tw

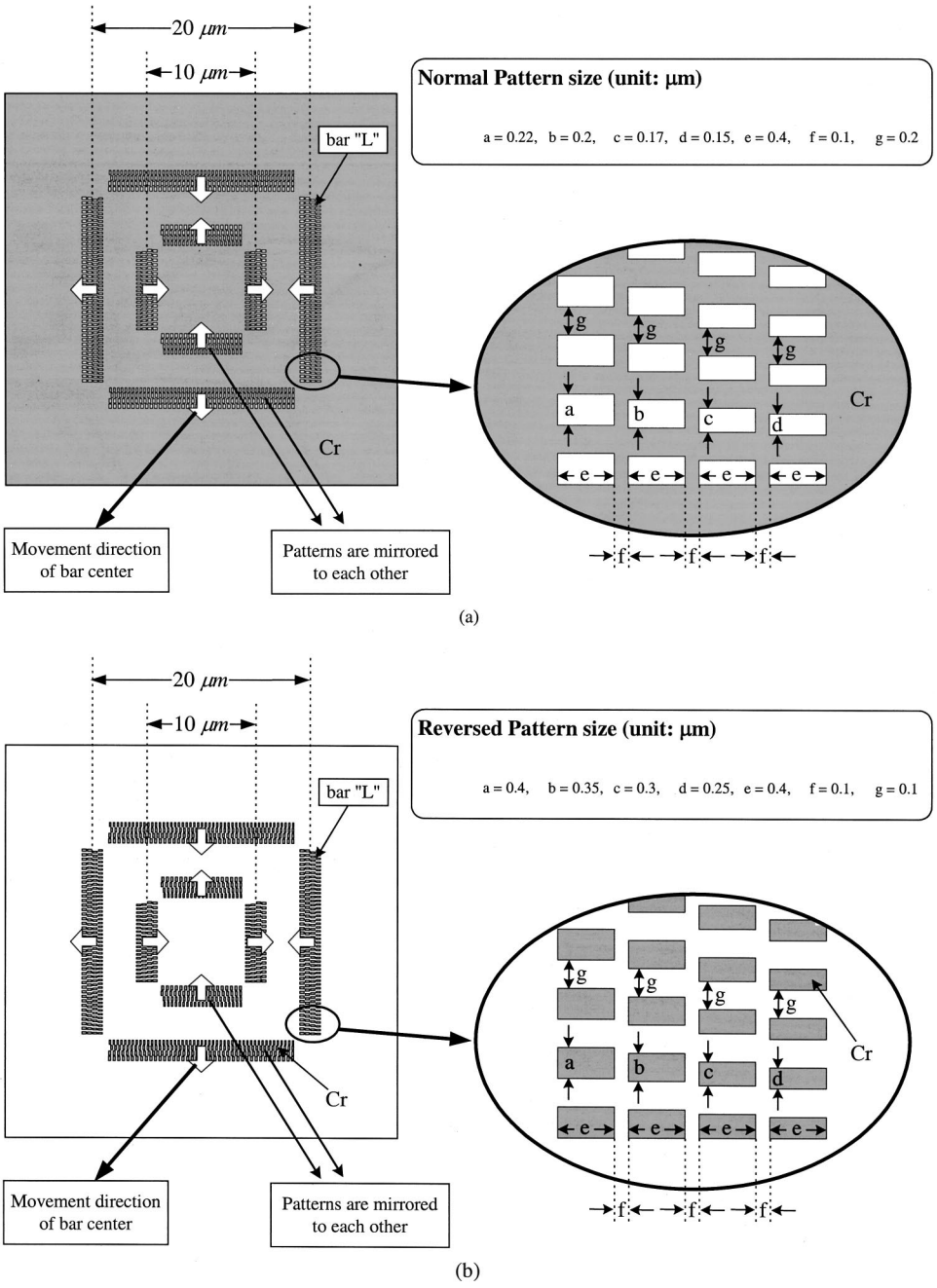

FIG. 1. Uniquely designed bar-in-bar patterns optimized to be best fitted by a second-order polynomial equation. (a) Normal pattern; (b) reversed pattern.

focus by using the opposite shifting direction of the inner and outer bars under defocus. The center-to-center shift (referred to herein as ''overlay shift'') of the inner and outer bars, which are mirrored to each other, are designed to be easily measured by an overlay measurement tool capable of determining the overlay shift by the center difference of inner and outer frames under various focus settings. The center of gravity of each bar moves under defocus due to the unique design of each bar, thereby causing the overlay shift. The BIB patterns were exposed by the FEM method to reveal the energy dependence of the overlay shift. The best way to determine the best focus position is to use a second-order polynomial equation to fit the measurement results. The bottom position (best focus) of the fitting curve is located at the point where the derivative is zero. The BIB pattern is distributed over the test reticle to measure features such as the focus, tilting, and field curvature for a stepper and a scanner.

B. Exposure conditions

Two photoresists are tested to ensure the application of the special BIB patterns: one for the contact hole pattern and the other for the line-and-space pattern. Here, photoresist refers to the photoresist of a contact hole unless specified otherwise. TEL Mark 8 is the track model used for resist coating and developing. The resists were coated onto silicon substrates that were hexamethyl disilazane (HMDS) vapor primed. The positive deep ultraviolet (DUV) resists were

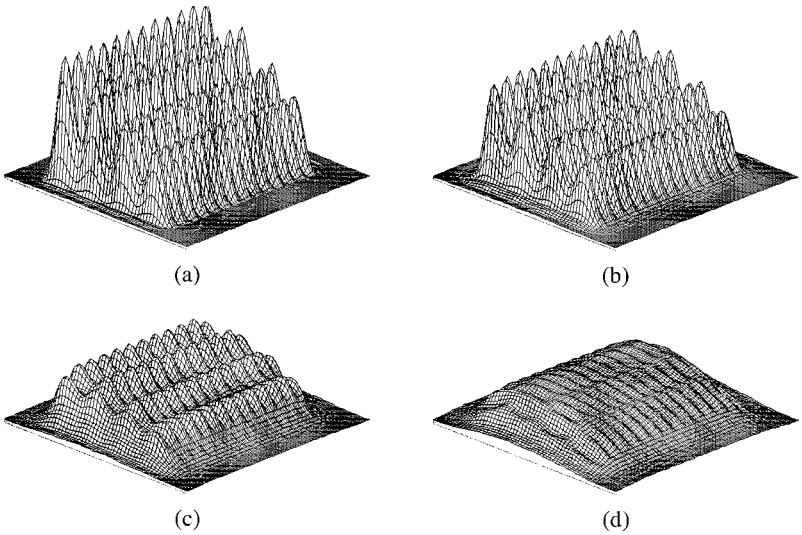

FIG. 2. Three-dimensional intensity profile of the BIB pattern under different focus settings: (a) best focus (F^*); (b) $F^*+0.4$ μm; (c) $F^*+0.8$ μm; (d) $F^*+1.2$ μm.

spin coated to 0.7 μm thickness and prebaked for 90 s at 100 and 110 °C for contact hole resist and line-and-space resist, respectively. All patterns were exposed by a KrF excimer laser stepper with a 248 nm wavelength. In this study we employed the ASML stepper PAS5500/300 as an exposure tool. While the BIB pattern can be used for both scanners (such as the PAS5500/700) and steppers, we are most interested in steppers because a scanner uses the center portion of the lens, and therefore has a smaller field curvature problem. The illumination system was set to a conventional mode, with a 0.57 NA and a 0.75 σ (partial coherence). The NA and sigma settings are set to be the same as the ones used for the standard machine acceptance test, since they have no special requirements. Postexposure bakes (PEBs) were performed the same as for the prebaked conditions for both resists. The resist films were developed in a 2.38 wt % tetramethylammonium hydroxide (TMAH)-based developer for 60 s. Designed to measure the layer-to-layer shift error, a metrology tool, the KLA5200, was used to measure the center-to-center shift of the inner and outer bars. A Hitachi S-9200 SEM was used to monitor the behavior of the bar under various focus and energy settings. Here, the optimized exposure energy, 49 mJ/cm^2, is selected to be approximately four times that of the "energy to clear," E_0 ($E_0 \sim 12$ mJ/cm^2), to yield the best performance.

III. RESULTS AND DISCUSSION

A. Effect of exposure energy on focus determination

1. Simulation, PROLITH/2

A simulation tool, PROLITH/2, is adopted to analyze the behavior of the novel BIB pattern. Figures 2(a)–2(d) display three-dimensional intensity profiles of the BIB pattern under different focus settings. The intensity profiles appear to become smoother when the wafer moves away from the best focus position, i.e., it becomes defocused. Figure 3 shows a comparison of a SEM picture and a simulated two-dimensional image profile for normal and reversed BIB pat-

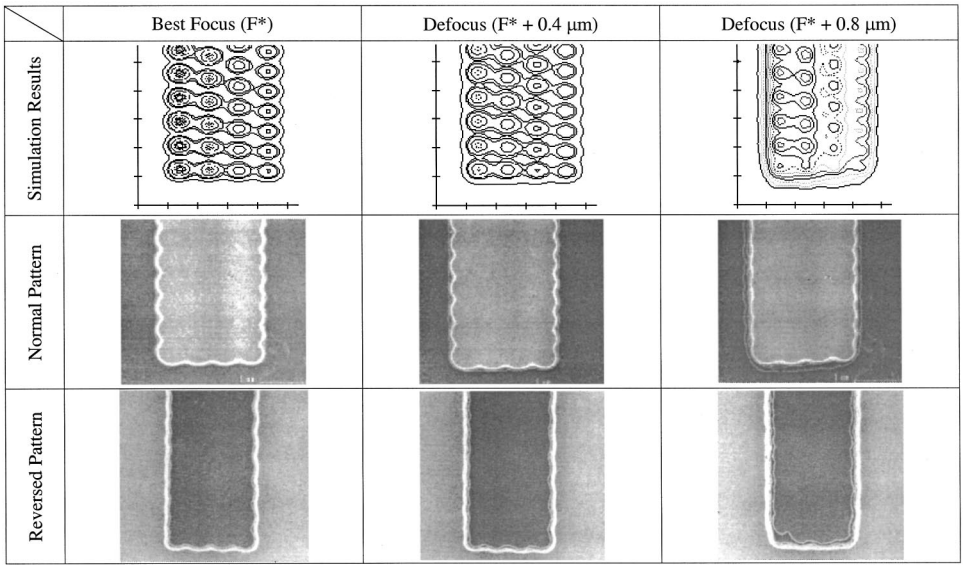

FIG. 3. Comparison of SEM pictures and simulated two-dimensional image profiles for normal (49 mJ/cm^2) and reversed (15 mJ/cm^2) BIB patterns under various focus settings.

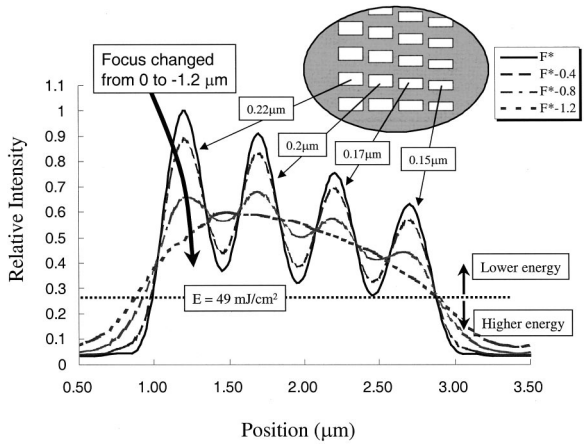

FIG. 4. Average intensity (PROLITH/2) profile along with the bar for best focus (F^*) and other focus settings, F^*, of 0.4, 0.8, and 1.2 μm.

terns. The close relationship validates the above discussion. The SEM pictures of the BIB pattern were obtained under the energy levels of 49 and 15 mJ/cm^2 for the normal and reversed BIB patterns, respectively. The small cavities found around the best focus become rounded when they are defocused. Due to light diffraction, the image becomes blurred and overlaps adjacent patterns, thus rounding the edge of the bar. Note that the small cavities do not influence the measurement results because the overlay measurement tools take the center of gravity of the bar. Here, the average signal of the center 80% of the bar length is adopted to avoid the noise information. Hence, the average intensity along with the bar is of particular interest.

In the following discussion, we will focus on the normal BIB pattern first, then discuss the reversed BIB pattern in Sec. III B. Figure 4 illustrates the intensity distribution, which is obtained by averaging the simulated intensity profile (by PROLITH/2) along with the bar, for the best focus (F^*) and other focus settings. In Fig. 4, the horizontal dashed line represents the level of exposure energy. The region in which the intensity is higher than the dashed line can be resolved by developer solution. The dashed line moves up (or down) if the lower (or higher) energy is used. According to our previous results,[1] the energy to acquire the zero shift on the side of smaller holes (right portion of Fig. 4) is about 49 mJ/cm^2. The center position shift of the bar was calculated based on this energy. The overlay shift obtained from the simulation and the measurement results (in the horizontal direction) are shown in Fig. 5. This close correlation again proves our assumption.

2. Employing the BIB pattern on the production wafers

As previously demonstrated,[1] only one of the exposure energies, 49 mJ/cm^2, is used to verify the overlay shift. Due to the optical proximity effect (OPE), printing zero bias (which means the pattern size on the wafer level is equal to the mask size divided by the lens reduction ratio) of different pattern size requires different energies. The energy level is normally selected to print the most critical pattern size on the target value, unless the OPC is applied. If the proposed BIB pattern is inserted into the scribe lanes to monitor the focus level of each monitor point, the performance of various energy levels should be verified.

In this study, a 0.2 μm isolated contact hole is selected to be the target's critical dimension (CD). Figure 6 illustrates the FEM outcome for five energy levels, 46, 49, 52, 55, and 58 mJ/cm^2. Evidently, 50 mJ/cm^2 is a good selection with which to correctly print the hole size, with an acceptable 0.8 μm DOF based on the criterion of $\pm$10% of target CD (ranging from 0.18 to 0.22 μm). The usable DOF of the 0.2 μm isolated contact hole is also shown in Fig. 6. Based on the DOF of the 0.2 μm isolated contact hole, the best focus setting will be selected as 0.1 μm to obtain a larger focus window. A range of $\pm$5% exposure latitude (EL) is normally required to print the pattern size within specifications of machine fluctuation. Notably, the energy is occasionally raised or lowered to print another pattern on the target size based on

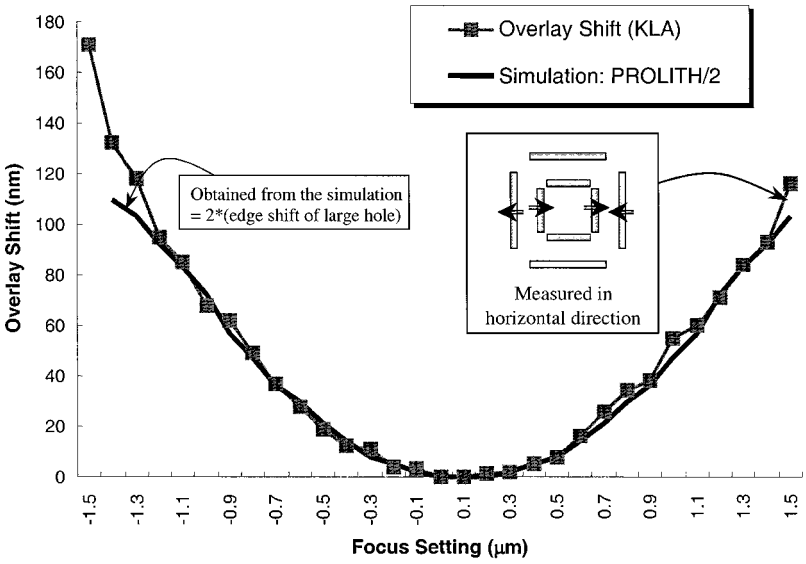

FIG. 5. Overlay shift obtained from the simulation (by PROLITH/2) and the overlay measurement results (by the KLA 5200 metrology tool).

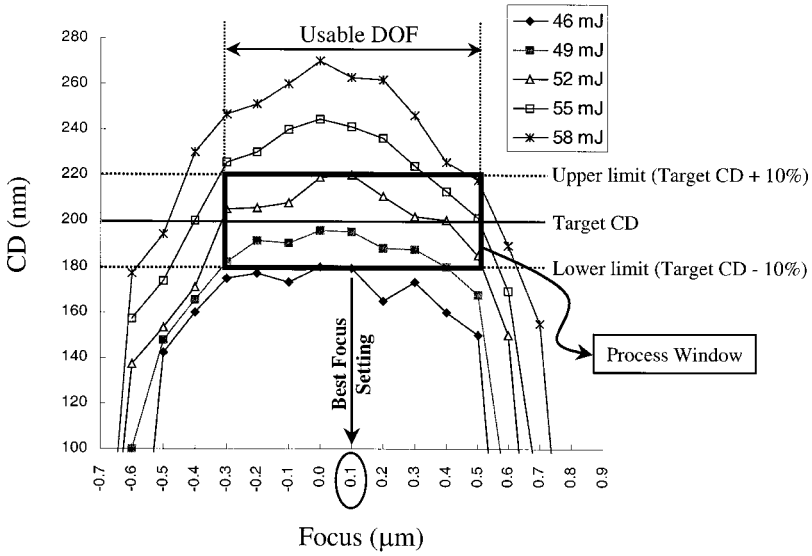

FIG. 6. CD result of 0.2 μm isolated contact hole for five energy levels (46, 49, 52, 55, and 58 mJ/cm^2). The energy level of 50 mJ/cm^2 is selected as the exposure energy for production to prevent the energy variation induced CD shift.

the device performance analyzed. This energy shift is normally less than $\pm 5\%$ of the original exposure energy. By combining these two factors, the final exposure energy will be within $\pm 10\%$ of the original energy of 50 mJ/cm^2, i.e., from 45 to 55 mJ/cm^2.

3. Verification of the working range of the novel BIB pattern

Evidently the novel BIB pattern should function properly within a range of 10 mJ/cm^2 to acquire related focus information during production. In this study, a wider energy range from 40 to 67 mJ/cm^2 is verified. Figure 7 displays the overlay shift of the BIB pattern for four energy levels, 40, 49, 58, and 67 mJ/cm^2. The exposure energy ranges from 3.3 to 5.6 times E_0. Obviously, the overlay shift is more sensitive to the distance from the best focus when the exposure energy is low. The curve is distorted from the ideal second-order polynomial equation when the energy is continuously lowered; meanwhile, increasing the energy flattens the curve and decreases the sensitivity to the focus shift. Figure 8 displays SEM pictures of different energies, 31, 40, 49, and 58 mJ/cm^2, at the best focus. Obviously, the residual photoresist between holes can induce measurement error and reduce the stability. Although some photoresists remain inside the bar for 40 mJ/cm^2, the experimental results in Fig. 7 confirmed that the overlay performance is still acceptable even when the energy is as low as 40 mJ/cm^2. All of the SEM pictures in Fig. 8 were taken at the best focus, and the energies are substantially higher than the energy to clear, E_0. Under defocus larger than 0.3 μm, the residual photoresist does not appear for energy of 40 mJ/cm^2, due to the nature of light diffraction. Therefore, the performance of the BIB pattern is still acceptable when the energy level is as low as three times that of E_0.

Finally, the best focuses were determined based on the previously stated derivative technique of fitting second-order polynomial curves. The derivatives of different energy levels are also shown in Fig. 7. The calculated best focuses for 40,

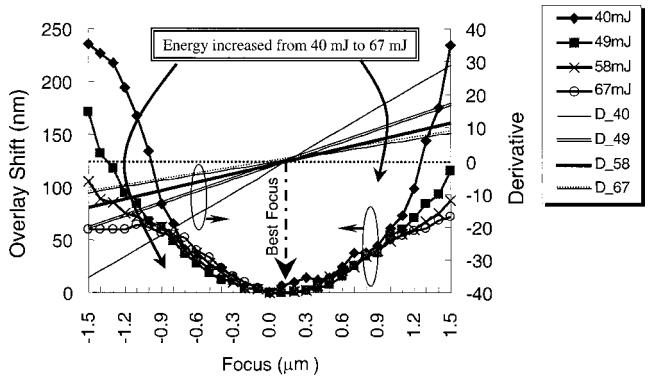

FIG. 7. Overlay shift and derivative of the fitting curve under different energy levels (40, 49, 58, and 67 mJ/cm^2).

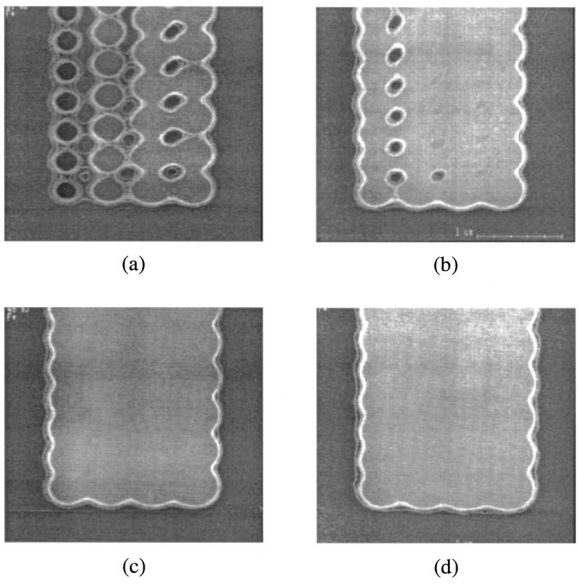

FIG. 8. SEM pictures of the bar of the novel BIB pattern with different exposure energies at best focus: (a) 31; (b) 40; (c) 49; (d) 58 mJ/cm^2.

49, 58, and 67 mJ/cm^2 are 0.103, 0.104, 0.098, and 0.095 μm, respectively, and they are nearly the same as the best focus setting, which is determined by the usable DOF of the 0.2 μm isolated contact hole. Therefore, the best focuses determined by these four energy levels are located almost at the same position for both higher and lower energy conditions. Based on the original energy, 50 mJ/cm^2, the usable EL of the BIB pattern is larger than $\pm$20%. Therefore, the proposed BIB can definitely be used for focus monitoring during production.

B. Reversed pattern design for line-and-space photoresists

Here in Sec. III B, we extend application of the BIB pattern from contact hole to line-and-space patterns. As is well known, the exposure energy for a contact hole pattern is higher than the energy of a line pattern. For the contact hole pattern, the exposure energy is approximately four times that of E_0. Therefore, the residual resist between the holes can be removed for the BIB pattern and a stable overlay shift can be obtained. However, this BIB pattern cannot be applied to the line-and-space pattern because of its substantially lower exposure energy. According to our results, the photoresist (for the line-and-space pattern) has an E_0 of about 8 mJ/cm^2. The energy required to expose a 0.2 μm zero biased line-and-space pattern is 16 mJ/cm^2, i.e., twice that of E_0.

A reversed BIB pattern was tested for the line-and-space photoresist. The original BIB pattern shown in Fig. 1(a) was designed to cover the entire reticle by chrome film, and only exposure light was allowed to pass through the holes in the bar. The reversed BIB pattern shown in Fig. 1(b) has the same layout as the original one. The only difference is that the hole areas are covered by chrome film and the other areas are transparent in order to let light pass through. Therefore, each bar contains various size resist islands instead of holes. Although the process window of the contact hole and lines and space are different, the $\pm$10% EL is a generally accepted value, and is used in the following discussion. Our results indicated that the overlay outcome of the original pattern sizes will not work very well for the reversed BIB pattern because the developer will remove some of the resist within the resist island. Therefore, the new combination [listed in Fig. 1(b)] was used for verification due to its smaller gap ($g=0.1$ μm) between resist islands and larger pattern size ($a-d$). To cover the required EL, the BIB pattern should function from 14.4 to 17.6 mJ/cm^2. Figure 3 displays SEM pictures of the reversed BIB pattern for different focus settings. The photoresist between small islands cannot be removed by developer solution unless the exposure energy is higher than about 20 mJ/cm^2 (again, this is a property of light diffraction). Hence, the small islands are connected to each other and become a resist bar pattern. During defocus, the gravity center shifts of inner and outer bars closely resemble those of the original BIB pattern. These overlay shifts can be measured by the overlay measurement tools as well. The overlay performance of the reversed BIB pattern is similar to the performance of a contact hole resist, such as the one in Fig. 7. Therefore, the best focuses determined by energies of 12, 15, and 18 mJ/cm^2 are 0.094, 0.107, and 0.101 μm, respectively. Therefore, we conclude that the reversed BIB pattern can cover EL of $\pm$18.75%. Similar to the BIB pattern for contact holes, the reversed BIB pattern can also be successfully employed during production of line-and-space patterns.

IV. APPLICATION

A. Monitoring the performance of exposure tools

In his study we have demonstrated that the BIB pattern can precisely determine the best focus by exposing a FEM. Only one point in the exposure field is needed to monitor the day-to-day focus drift. Although a 0.6 μm or larger DOF is normally a minimum requirement for mass production, the DOF for a specific pattern is generally smaller than 0.6 μm. This is because a reticle pattern smaller than the machine's capability is always used in order to lower the user's cost of ownership (COO). The field curvature (the focal plane deviation of the exposure field) of the lens may be as large as 0.3 μm for an advanced stepper, and the remaining focus budget inside the exposure field can be squeezed to smaller than 0.3 μm. Therefore, precisely determining the best focus, tilting, and field curvature of the exposure tool is increasingly important. On the production line, the monitoring frequencies of best focus, tilting, and field curvature are normally daily, weekly, and quarterly, respectively. The tighter the focus budget the higher monitor frequency needed. Raising the monitor frequency leads to a higher cost for machine time. Therefore, there is a trade-off between machine focus position accuracy and machine time.

1. Obtaining the focus value at an exposure field

Conventional focus monitor methods, such as focus dot arrays and FEM, only measure one focus point in the field. This method cannot reveal the conditions of tilting and field curvature. Alternatively, the BIB pattern proposed here solves the previous problem. By using the test reticle, a FEM result can be obtained by inserting the test wafer into the processing wafers without affecting the production line. After the wafer is developed, the overlay shift of the BIB patterns can be obtained by an off-line overlay measurement tool. If five points (the center and four corners) of focus are determined by the BIB pattern, tilting of the exposure field can be obtained. In addition, the BIB patterns are measured by an off-line metrology tool, and it takes only 3 min to do it. The field curvature is normally shaped like a bowl, and does not need to be frequently measured. Based on the focus values at five measurement points (the center and four corners), the best focus position of the exposure field can be determined in a more precise manner, such as best focus (BF) = [center + (four corners) / 4] / 2. Therefore, we conclude that the BIB pattern can be routinely used to accurately and efficiently monitor the focus conditions of exposure tools.

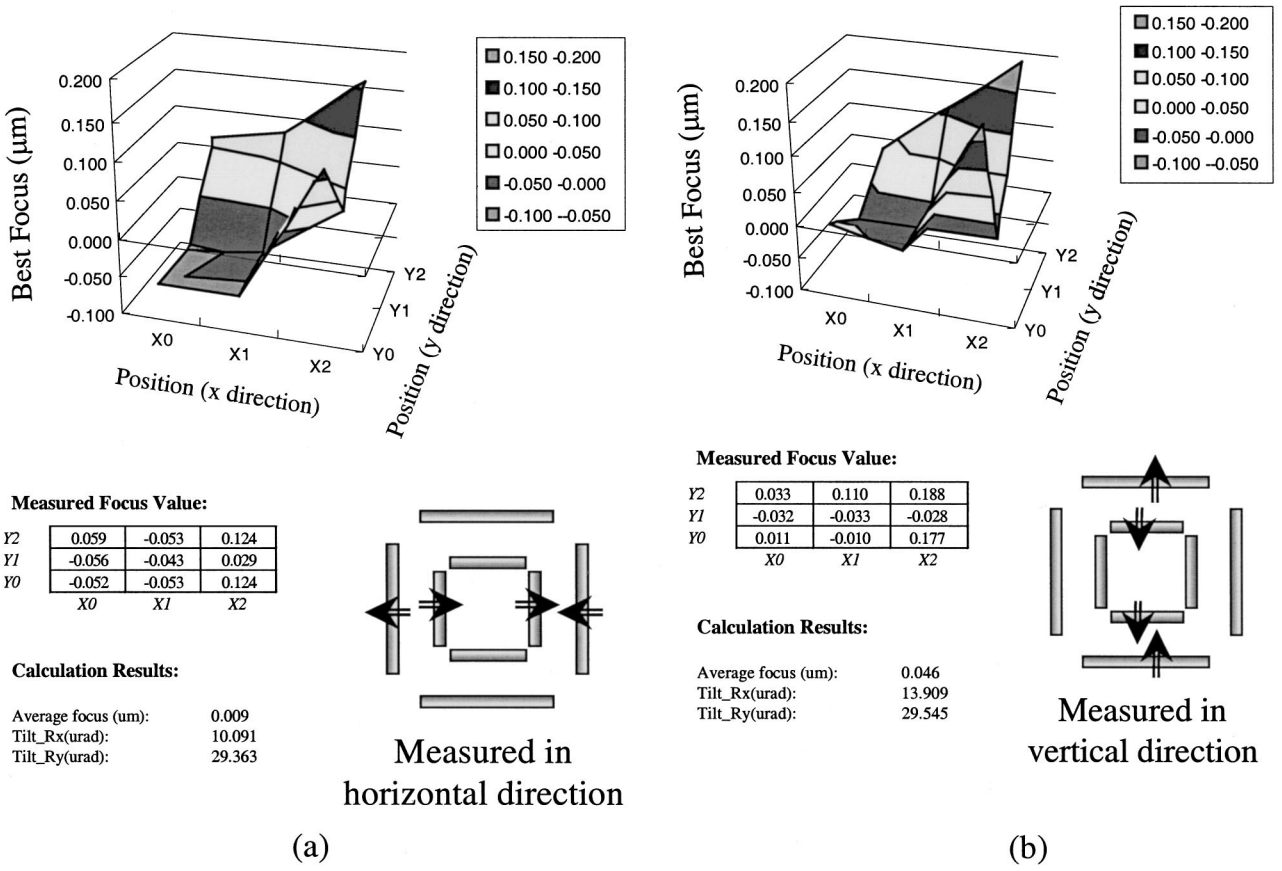

FIG. 9. Figures and nine measured focus values (a) in the x direction: F_h^* and (b) in the y direction: F_v^*. The tilting values of Rx and Ry are shown.

2. Measuring the astigmatism by the novel BIB pattern

The inner and outer bars shift both horizontally and vertically when the BIB pattern is defocused; when there is astigmatism, at each BIB located position, there are two best focus values: horizontal (F_h^*) and vertical (F_v^*). The astigmatism can be obtained by simply subtracting the best focus F_h^* from F_v^*. The focus measurements are performed at nine points (the center, four corners, and four sides) to accurately determine the tilting of the exposure field. Figures 9(a) and 9(b) display the horizontal and vertical best focus values at the nine positions (three in x by three in y: labeled X0–X2 in the x direction and Y0–Y2 in the y direction), covering the whole exposure field. The focus value measured at the center of exposure field (X1, Y1) in the horizontal direction (F_h^*) is -0.043 μm. The average focus value at the nine measurement points {BF = [center + (four corners) + (four sides)] / 9}, is 0.009 μm. A 0.052 μm focus difference is present between the conventional one point focus value and the average focus value of the exposure field. Similarly, the average focus value in the vertical direction (F_v^*) is 0.046 μm (the best focus at the shot center is – 0.033 μm). Figures 9(a) and 9(b) also give the tilting values of Rx and Ry. Figure 10 summarizes the astigmatism results ($F_h^* - F_v^*$).

B. Leveling performance improvement

1. Resist profile deformation under defocus

The novel BIB pattern can be used to prevent the resist's top loss and scumming induced by poor flatness of the wafer

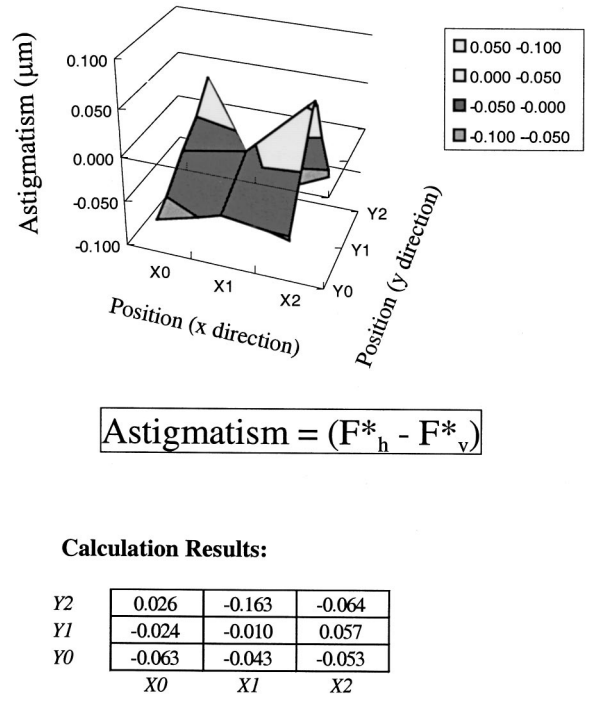

FIG. 10. Astigmatism within an exposure field obtained by calculating the focus difference in the x and y direction: $(F_h^* - F_v^*)$.

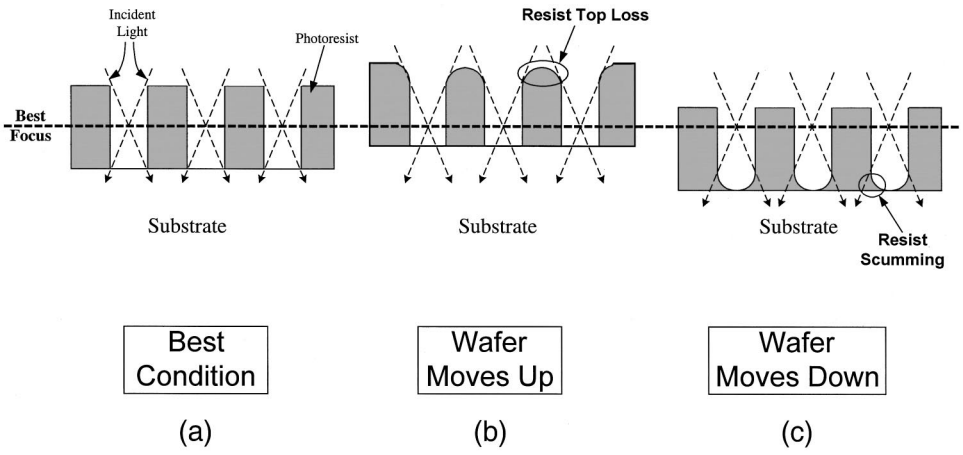

FIG. 11. Impact of the wafer position on the resist profile: (a) best condition, (b) wafer moves upward, and (c) wafer moves downward.

topography. Figure 11 presents a schematic of the resist performance under different defocused conditions. Figure 11(a) shows a wafer located at the best focus position. If the wafer moves toward the lens, the top portion of the resist will be exposed by diffracted light and removed by developer solution [as shown in Fig. 11(b)]. If the wafer is moved away from the lens, the bottom of the resist profile may become scummed [Fig. 11(c)]. The reasons for these occurrences are as follows. (1) Incident light loses its energy when it passes through the resist. (2) The incident light is spread out at the bottom of resist, and is therefore less intense. Some residual resist cannot be removed by developer solution because of the lower intensity at the bottom corners of resist, which induces the scumming problem.

2. Film thickness variation induced focus problem

Normally, the step height induced by film stacking increases the difficulty of correctly printing the patterns on the lower and upper regions. Figure 12 presents an illustrative example of the step height issue, which is typically observed in the dynamic random access memory (DRAM) process. Because of the film stack, the cell region is higher than that in the periphery region. Therefore, the step height reduces the limited focus budget of exposure tools. Although exposure tools can perform leveling and height adjustment for each exposure shot, the wafer topography problem still cannot be solved. The inability to solve this problem is due to the fact that the leveling system takes the average height of the exposure field as a target and adjusts the wafer chuck to fulfill the requirement. The cell area occupies most of the area of a chip, accounting for why the leveling system can only optimize the condition of the cell area. The focus setting is normally determined during the pilot run to yield good performance for the cell and periphery region. However, the step height may have wafer-to-wafer or lot-to-lot fluctuation and, because of this, causes a focus problem for the periphery region.

3. Asymmetrical layout induced improper leveling adjustment

Another leveling problem is caused by the asymmetry distribution of a cell and its periphery. Figure 13 illustrates how improperly adjusting the leveling system affects the product. One exposure shot containing six chips (3×2) is shown in Fig. 13(a), in which the cell area is located on the left side of each chip, leaving most of the peripheral area on the right

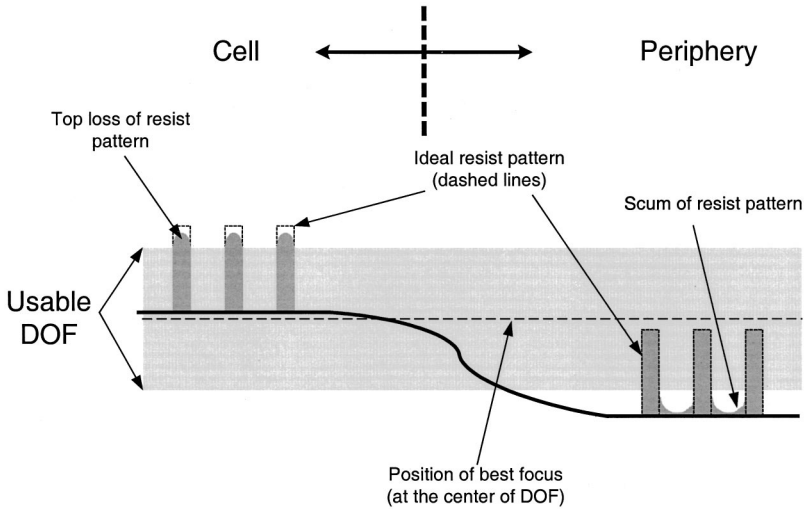

FIG. 12. Step height induced scum and resist top loss issues. This is normally observed at the cell and periphery regions in the DRAM process.

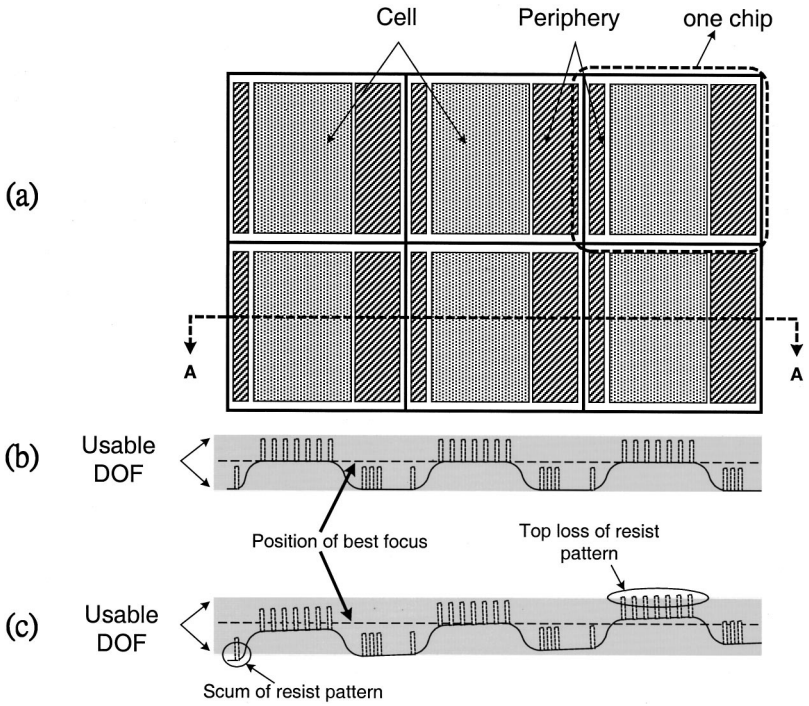

FIG. 13. Improper leveling adjustment induced scum and top loss problems of production wafers due to the asymmetry distribution of a cell and its periphery.

side. A cross section in the *x* direction, **AA**, is shown in Fig. 13(b), which has been ideally leveled. To simultaneously correctly print the cell and periphery patterns, the focus setting at the middle of the cell and periphery [denoted as ''position of best focus'' in Fig. 13(b)] is selected, due to the limited DOF of the patterns. The leveling system normally scans the entire field and tilts the wafer to obtain the minimum height difference in the exposure field. Figure 13(c) displays the cross section after leveling adjustment. Clearly, the cell pattern on the right side of the exposure field may suffer from the top loss issue, and the small portion of the periphery on the left side may encounter a scum problem.

Although recent improvements have been made in providing a user defined tilting adjustment option to overcome the topography issue, top loss and scum problems still frequently occur in factories for the following reasons: (1) the DOF is limited; (2) the step height has continuously increased; and (3) the focus and tilting control are not totally accurate. The scum can cause a space CD change, which is highly sensitive to the focus shift. However, the top loss percentage cannot be quantitatively measured by an in-line SEM, and the resist loss reduces the etching resistance and induces broken lines. In factories, device function failure caused by top loss and scum problems can be prevented in two ways: (1) add the SEM measurement at the cell (right side) and the periphery (left side); and (2) move the focus setting upward to prevent top loss. The disadvantages of these two are throughput loss and reduction of the process window of the periphery patterns. To overcome these problems, we can place two sets of BIB patterns in each scribe lane (two sets in the scribe lane to the left of the chip, and two more in the scribe lane to the right of the chip) to correct leveling misadjustment. We must also arrange the processing so that one of the two sets of patterns in each scribe lane is on the same film stack as the cells, and the other set is on the same film stack as the periphery. At the position of best focus (shown in Fig. 13), both the cell and periphery patterns are slightly out of focus. The ''best'' overall focus occurs when both patterns are equally defocused. In this case, any deviation from best focus results in one pattern having a larger overlay shift than the other one. The direction of the focus error is known since it is also known that the cell pattern is above the position of best focus and that the periphery pattern is below. Therefore, this focus error can be fed back to the exposure tool to obtain a more accurate focus and tilt adjustment.

The chemical mechanical polishing (CMP) process has been used extensively to reduce the step height recently, despite its relatively high cost and complexity. However, the non-CMP process is still widely used for production technologies that have lower requirements, e.g., larger than a 0.35 μm process, to reduce wafer cost.

C. Related applications

As is well known, light heats the lens during exposure, and therefore causes focus drift. Due to the high intensity of *I*-line exposure, the impact of lens heating on focus variation during wafer processing can no longer be neglected. Therefore, many models have been established to describe the behavior of focus drift.[26] Among the factors influencing the lens heating correction are the reticle transmission factor, exposure energy, and wafer shot number. The parameters of the model equation must be precisely determined to compensate for the lens heating induced focus drift.

Normally, parameter determination is first performed on a focus measurement reticle, such as the previously mentioned focus dot arrays reticle, with known reticle transmission and exposure energy. After a full lot of wafers (25 wafers) is

exposed, focus drift can be read by the exposed FEM on each wafer. Focus drift can then be fed back to the system to fine tune the model. After a trial and error procedure is completed, the required parameters can be found and put into the system. The lens heating correction should then be tested on the production wafer since there are different factors for various products. Then, a lot of production wafers are exposed and the wafers are sent to the SEM in order to measure the CD or profile. As mentioned earlier, it is difficult to determine the focus shift by SEM CD measurements because PR retains nearly the same linewidth or contact hole size over a wide range of defocus. Therefore, judging the focus condition on each wafer is extremely difficult, and leads to poor lens heating correction. The lens heating problem affects not only wafer-to-wafer focus, but also shot-to-shot focus. Using the CD or pattern profile to fine tune the lens heating correction is time consuming and inaccurate.

The BIB pattern, which is inserted for focus and tilt monitoring, can also be employed to fine tune the lens heating correction. The BIB pattern can quantitatively determine the focus value for each shot and wafer to accurately compensate for the effect of lens heating. Another merit of the BIB pattern is its convenience in light of the fast off-line measurement speed. In addition, the focus values on each shot and wafer can be easily obtained.

The BIB pattern can also be applied to other areas such as individually changing the focus or tilt at edge dies, monitoring wafer chuck flatness, and retaining the accuracy and time-saving properties.

V. CONCLUSION

In this study we have presented a uniquely designed bar-in-bar pattern that is drawn on a conventional chrome binary mask. Experimental results demonstrate the capability of the proposed BIB to provide fast accurate focus related information of lithographic tools by measuring off-line metrology tools. Inserting the BIB pattern into the scribe lanes of the production mask can obtain the focus, tilt and other focus related information. This BIB can also be extended to obtain other useful information, such as lens heating correction, edge die leveling adjustment, and wafer chuck flatness.

ACKNOWLEDGMENT

The authors would like to thank the National Science Council of the Republic of China for financially supporting this research under Contract No. NSC 88-2215-E009-045.

[1]C. Y. Ku, T. F. Lei, J. M. Shieh, T. B. Chiou, and Y. C. Chen, Proc. SPIE **4182**, 268 (2000).
[2]T. A. Brunner, J. Lewis, and M. Manby, Proc. SPIE **1201**, 286 (1990).
[3]M. van den Brink, H. Franken, S. Wittekoek, and T. Fahner, Proc. SPIE **1261**, 298 (1990).
[4]T. E. Adams, Proc. SPIE **1464**, 294 (1991).
[5]A. Starikov, Proc. SPIE **1261**, 315 (1990).
[6]W. H. Arnold and H. J. Levinson, Proc. SPIE **772**, 21 (1987).
[7]J. W. Gemmink, Proc. SPIE **1088**, 220 (1989).
[8]T. A. Brunner and R. R. Allen, IEEE Electron Device Lett. **6**, 329 (1985).
[9]T. A. Brunner and R. R. Allen, Proc. SPIE **565**, 6 (1985).
[10]C. P. Ausschnitt, Proc. SPIE **3677**, 140 (1999).
[11]S. Stalnaker, P. Leuhrmann, and J. Waelpoel, Microelectron. Eng. **21**, 22 (1993).
[12]A. D. Katnani and B. J. Lin, Proc. SPIE **1674**, 264–270 (1992).
[13]M. A. Levenson, N. S. Viswanathan, and R. A. Simpson, IEEE Trans. Electron Devices **ED-29**, 1828 (1982).
[14]H. Ohtsuka and T. Onodera, Proc. SPIE **1674**, 53 (1992).
[15]T. Terasawa, N. Hasegawa, T. Kurosaki, and T. Tanaka, Proc. SPIE **1088**, 25 (1989).
[16]Y. Liu, A. K. Phan, and A. Zakhor, Proc. SPIE **1674**, 14 (1992).
[17]W. H. Arnold, E. Barouch, U. Hollerbach, and S. A. Orszag, Proc. SPIE **1926**, 380 (1993).
[18]R. Budd, J. Staples, D. Dove, W. H. Arnold, E. Barouch, U. Hollerbach, and S. A. Orszag, Proc. SPIE **2087**, 380 (1993).
[19]T. A. Brunner, A. L. Martin, R. M. Martino, C. P. Ausschnitt, T. H. Newman, and M. S. Hibbs, Proc. SPIE **2197**, 541 (1994).
[20]D. Ziger and P. Leroux, Proc. SPIE **3677**, 194 (1999).
[21]K. Suwa, H. Tateno, N. Irie, and S. Hirukawa, Proc. SPIE **2440**, 712 (1995).
[22]Y. C. Kim, G. S. Yeo, J. H. Lee, H. Kim, and U. I. Chung, Proc. SPIE **3677**, 184 (1999).
[23]M. Watanabe, Jpn. J. Appl. Phys., Part 1 **32**, 5867 (1993).
[24]J. P. Kirk, Proc. SPIE **1463**, 282 (1991).
[25]R. P. Grosso and R. Crane, Jr., Proc. SPIE **1929**, 65 (1993).
[26]T. A. Brunner, S. Cheng, and A. E. Norton, Proc. SPIE **922**, 366 (1988).